Analysis of Mechanical Properties for the Heat Resistant Co-Modified 12 and 9% Cr Steels

A. E. Fedoseeva[a,]*, I. S. Nikitin[a], N. R. Dudova[a], and R. O. Kaibyshev[a]

[a]*Belgorod National Research University, Belgorod, 308015 Russia*
*e-mail: fedoseeva@bsu.edu.ru

Abstract—An analysis of mechanical properties has been performed for 12% Cr and 9% Cr steels by means of tension tests at 20 and 650°C and yield tests at 650°C and applied stresses of 200−100 MPa with a step of 20 MPa. The yield strength and ultimate tensile strength of the 12% Cr steel are, correspondingly, 614 and 710 MPa at 20°C and 365 and 390 MPa at 650°C. At both temperatures, the strength properties of the 12% Cr steel under tension are better than for the 9% Cr steel due to higher values of contributions from solid-solution hardening (+30 MPa) and substructural hardening (+23 MPa) to the room-temperature yield strength. The analysis of creep properties shows that the time to fracture at high stresses for the 12% Cr steel is much longer than for the 9% Cr steel due to a more prolonged transient creep stage and, at low applied stresses, there is almost no difference in the creep behavior of the 12% Cr and 9% Cr steels. The 1% creep limit estimated from the empirical dependence between the stress and the time required to attain the strain with a degree of 1% for the 12% Cr steel is 82 MPa, being comparable with the 1% creep limit of the 9% Cr steel.

Keywords: refractory steel of martensite class, tension tests, hardening mechanisms, creep, creep limit

DOI: 10.1134/S0031918X20120054

INTRODUCTION

The 9% Cr steels are suitable materials for boilers, steam pipelines, and turbine rotors of coal-fired thermal power plants because of their more stable structure during the process of creep compared to the 12% Cr steels [1]. The optimal steel for boiler tubes and steam pipelines is currently considered to be European steel P92 (0.1C−0.05N−9Cr−1.8W−0.6Mo−0.24V−0.07Nb), which allows prolonged operation at temperatures up to 600°C and short-life service up to 620°C [2−7]. All the new high-chromium steels are developed on the basis of the steel P92 by modifying its chemical composition [1, 3−9]. The cobalt addition of 3% to the steel P92 essentially increases its long-term strength from 72 to 86 MPa, which is calculated with the Larson−Miller parameter at a test temperature of 650°C on the basis of 100 000 h [9].

However, the 9% Cr steels are limited in application at temperatures above 630°C despite their high creep resistance. This is because the chromium content of less than 11% does not provide sufficient resistance to oxidation. The formation of wustite FeO at a temperature of nearly 637°C on the surface of parts manufactured of 9% Cr steels necessitates a special operation of preliminary surface oxidation for the formation of a protective Cr_2O_3 oxide film, which prevents the surface from oxidation under operation [1, 10]. To improve the resistance to oxidation, it is necessary to increase the chromium content up to 11−12%, as the 11% Cr steel requires no similar treatment; the refractory characteristics of the 11% Cr steel provide its service at 650°C due to a dense chromium oxide layer, which is formed in a natural way on the surface of this steel and provides its high refractoriness in an overheated steam atmosphere [1, 6]. However, the 12% Cr steels demonstrate lower creep resistance characteristics compared with the 9% Cr steels because of their microstructural instability under creep [1, 3−6].

To improve the microstructural stability of the 12% Cr steel under creep and, consequently, its creep resistance, the microstructural design of the 12% Cr steel was developed on the basis of earlier studies [7−9, 11] by optimizing the content of its austenite and ferrite-stabilizing elements. An increase in the chromium content to 12% in the studied steel as necessary to improve the resistance to oxidation up to 650°C in combination with a low nitrogen content was compensated by increasing the concentration of substituting austenite-stabilizing elements, namely, the boron content was increased to 0.01% with the addition of surplus copper and tantalum to 1 and 0.07%, respectively [11]. The corrected chemical composition of new steels has resulted in a δ-ferrite content of less than 10% in steel [11]. An increase in the boron content must decelerate diffusion-controlled processes like the climb of dislocations and the coarsening of secondary phase particles by the Ostwald ripening

Table 1. Chemical compositions of the studied 12% Cr and 9% Cr steels (in wt %)

Steel	C	Cr	Co	Mo	W	V	Cu	Nb	B	N	Ta
12% Cr	0.11	11.4	3.0	0.6	2.5	0.23	0.76	0.04	0.01	0.003	0.07
9% Cr	0.12	9.3	3.1	0.4	2.0	0.23	–	0.06	0.005	0.05	–

[1, 5]. The addition of copper is caused by the possible formation of nanoclusters of 3−5 nm in size under tempering, and these nanoclusters, being nucleation sites of Laves phases precipitating under creep, provoke a more finely-dispersed distribution of this phase [1, 5]. The addition of tantalum must provide the three-phase separation of Me(C,N) carbonitrides into niobium-rich Nb(C,N), vanadium-rich V(C,N), and tantalum-rich Ta(C,N) particles to decelerate the substitution of nanosized Me(C,N) particles by coarse Z-phase particles [12]. The complex effect of the mentioned doping elements must improve the microstructural stability of the 12% Cr steel and, consequently, increase its creep resistance. The objective of this study was to perform the analysis of mechanical properties under tension and creep at 650°C for the studied Co-modified 12% Cr steel in comparison with the 9% Cr steel.

METHOD

The chemical compositions of the 12% Cr and 9% Cr steels are given in Table 1. The 12% Cr steel was melted in Institut für Eisenhüttenkunde (IEHK) (Aachen, Germany) in a vacuum induction furnace. The 9% Cr steel was cast in NPO Central Research Institute of Mechanical Engineering Technology (Moscow, Russia) in a high-frequency induction furnace. The ingots were reforged into blanks shaped as bars of square cross section with a square side of 20 mm by free forging within a temperature range from 1150 to 900°C. The thermal treatment of the 12% Cr and 9% Cr steels consisted in normalization from 1070 and 1050°C with further tempering at 770 and 750°C for 3 h, respectively. Tension tests were performed on plane specimens with a working part length of 35 mm and a 7×3-mm^2 cross section surface area at room temperature and a temperature of 650°C and a strain rate of 2 mm/min. The plane specimens with a working part length of 25 mm and a 7×3-mm^2 cross section surface area and the cylindrical specimens with a working part length of 100 mm and a diameter of 10 mm were subjected to creep testing until failure at a temperature of 650°C and applied stresses ranged within 200−100 MPa with a step of 20 MPa on an ATS2330 lever arm testing machine.

Structural studies were performed on a JEM JEOL-2100 transmission electron microscope (TEM) equipped with an INCA energy-dispersive attachment for determining the local chemical composition of particles and the solid solution. TEM foils were prepared by electrolytic polishing in the electrolyte containing 10-% perchloric acid in acetic acid. The size of laths/subgrains was determined by the random linear intercept method with consideration for all the visible subboundaries from TEM images. The density of free dislocations inside laths/subgrains was estimated from the amount of points where dislocations emerged on the lower and upper surfaces of foil under the conditions of multibeam imaging with a high excitation vector. The methods were described in more detail in previous papers [7−9, 11].

RESULTS AND DISCUSSION

Structure of the 12% Cr and 9% Cr Steels after Thermal Treatment

Normalizing with the following tempering led to the formation of a tempered martensite lath structure in both steels. The structural parameters of the studied 12% Cr and 9% Cr steels after thermal treatment are given in Table 2.

The TEM images of the initial structure of the studied 12% Cr and 9% Cr steels are shown in Fig. 1. The initial structure has a strict hierarchical character: prior austenite grains are divided into blocks, which in turn are divided into packets composed of martensite laths. The average transverse size of martensite laths is nearly 300 nm for both steels (Fig. 1, Table 2). A high density of dislocations ($\sim 2 \times 10^{14}$ m^{-2}) was revealed inside martensite laths of both steels (Table 2). Cr, Fe, and W-rich $Me_{23}C_6$ carbide particles are on the boundary of prior austenite grains, packets, blocks, and martensite laths (Fig. 1). The average size of $Me_{23}C_6$ particles on the boundaries of prior austenite grains and martensite laths is nearly 55 and 90 nm (Table 2) for the 12% Cr and 9% Cr steels, respectively. An essential structural distinction between the studied steels consists in the composition of Me(C,N) carbonitrides. In the 9% Cr steel, Me(C,N) particles sustain two-phase separation into vanadium-rich V(C,N) particles with an average size of 20 nm and niobium-rich Nb(C,N) particles with an average size of 40 nm (Fig. 1b, Table 2). In the 12% Cr steel, M(C,N) particles also sustain two-phase separation into niobium-rich Nb(C,N) particles with an average size of 40 nm and tantalum-rich Ta(C,N) particles with an average size of 50 nm (Fig. 1a, Table 2). The volume fraction of these particles was estimated by Thermo-Calc software (Table 2). The solid solution of the 12% Cr steel after tempering at 770°C has the following composition (wt %): Cr, 10.5; Co, 3.0; W, 2.1; Mo, 0.5; V, 0.2. The composition

Table 2. Structural parameters of the 12% Cr and 9% Cr steels after thermal treatment

Parameters	12% Cr steel	9% Cr steel
Size of laths, nm	0.29 ± 0.05	0.34 ± 0.05
Number density of dislocations, m^{-2}	2.0×10^{14}	2.0×10^{14}
$Me_{23}C_6$ size, nm	55 ± 5	90 ± 5
$Me_{23}C_6$ content, vol %	2.25	1.96
Nb(C,N) size, nm	40 ± 5	40 ± 5
Ta(C,N) size, nm	50 ± 5	–
V(C,N) size, nm	–	20 ± 5
Me(C,N) content, vol %	0.08	0.25

of the solid solution of the 9% Cr steel after tempering at 750°C is the following (wt %): Cr, 8.2; Co, 3.0; W, 1.8; Mo, 0.4.

Mechanical Properties under Tension

The engineering tension curves measured for the studied 12% Cr and 9% Cr steels by uniaxial tension testing at room temperature and a temperature of 650°C are plotted in Fig. 2. The 12% Cr steel demon-strates an increase in the yield strength and ultimate tensile strength at both temperatures of testing in comparison with the 9% Cr steel. Thus, the yield strength of the 12% Cr steel is 10 and 23% higher than $\sigma_{0.2}$ if the 9% Cr steel, and the ultimate tensile strength of the 12% Cr steel is 1.5 and 20% higher than σ_u of the 9% Cr steel after tension tests at 20 and 650°C, respectively (Table 3).

Hardening Mechanisms

To ascertain the reasons for a higher strength of the 12% Cr steel, the contributions of different hardening mechanisms to the overall strength were calculated in a similar way to the calculations [11]. The hardening types taken into account were the following:

—Hardening due to lattice friction σ_0 [13];

—Work hardening σ_{WH} [14];

—Solid-solution hardening by substitution elements σ_{ss} [15];

—Dislocation hardening by the Taylor model σ_{disl} [16];
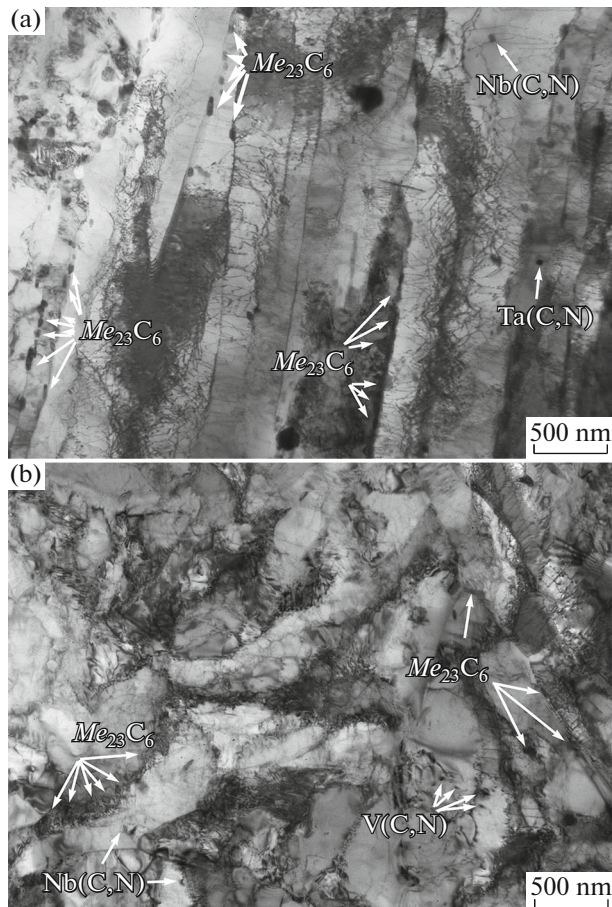
Fig. 1. Lath structure of troostomartensite in the studied (a) 12% Cr and (b) % Cr steels.
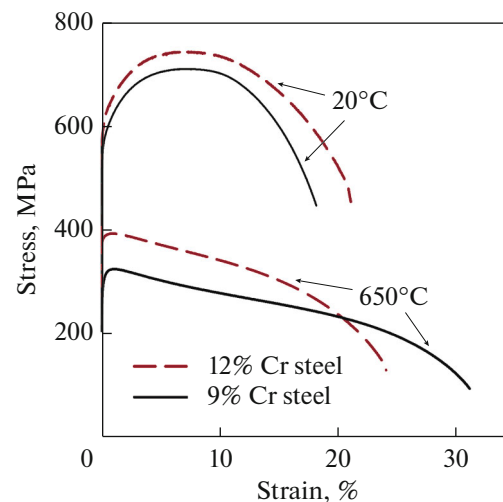
Fig. 2. Engineering tension curves of the studied 12% Cr and 9% Cr steels.

Table 3. Properties of the 12% Cr and 9% Cr steels under tension at 20 and 650°C

Properties	12% Cr steel	9% Cr steel
Testing at 20°C		
Creep limit, MPa	614	560
Ultimate strength, MPa	710	700
Elongation, %	21	19
Testing at 650°C		
Creep limit, MPa	365	296
Ultimate strength, MPa	390	325
Elongation, %	25	32

—Precipitation hardening according to the Orowan equation modified by F.J. Humphreys [17] under the assumption that all the particles are uniformly distributed over the matrix volume σ_{part}; and

—Substructural hardening by subgrains with low-angle boundaries by the Langford—Cohen model σ_{lath} [18, 19].

The results of calculations are shown in Fig. 3.

The analysis of contributions from different hardening mechanisms to the overall strength has demonstrated that an increase in the yield strength of the 12% Cr steel under tension testing at room temperature in comparison with the 9% Cr steel is provided by the growth of

—Solid-solution hardening due to a higher Cr, W, and Mo content in the solid solution after thermal treatment (+30 MPa) and

—Substructural hardening by subgrains due to a smaller transvere size of martensite laths (+23 MPa).
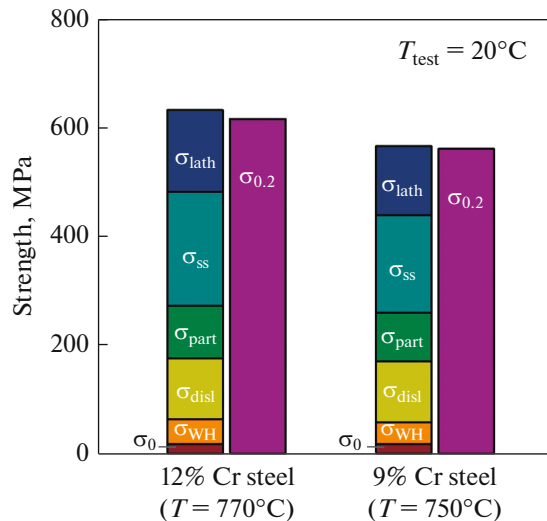

Fig. 3. Comparison of contributions from different hardening mechanisms to the overall strength of the studied 12% Cr and 9% Cr steels; $\sigma_{0.2}$ is the creep limit under tension at 20°C.

Let us note that, despite the essential distinctions between the morphology and sizes of secondary phase particles in the 12% Cr and 9% Cr steels, the values of precipitation hardening in both steels are almost the same. In the 12% Cr steel, a great contribution to precipitation hardening from fine $Me_{23}C_6$ carbide particles compensates a smaller contribution from $Me(C,N)$ carbonitrides, whose low volumetric content is caused by a decrease in the nitrogen content (see Table 1 and 2). Hardening due to lattice friction forces, work hardening, and dislocation hardening also have the same values for both steels (Fig. 3).

Mechanical Properties under Creep

The dependences of the creep rate on the degree of strain and time at a temperature of 650°C and applied stresses of 180 and 100 MPa for the studied 12% Cr and 9% Cr steels are shown in Fig. 4.

An essential distinction in the behavior of the studied steels is a more prolonged transitional stage of creep in the 12% Cr steel at a high applied stress of 180 MPa (Fig. 4b). At the transient creep stage, the creep rate continuously decreases as a result of hardening until a minimum creep rate is attained. This state corresponds to the establishment of equilibrium between the material hardening and softening processes [1, 3]. Softening at the transient creep stage predominantly occurs due to the redistribution of dislocations [1, 3]. A more highly doped solid solution and a smaller width of martensite laths in the 12% Cr steel (Fig. 3) with a resulting increase in the tension strength in comparison with the 9% Cr steel provide a higher resistance to the softening processes at the transient creep stage, as there are a greater number of obstacles for the motion and rearrangement of dislocations. Moreover, the minimum creep rate in the 12% Cr steel at a high stress is nearly two orders of magnitude lower than in the 9% Cr steel (Figs. 4a and 4b). A decrease in the applied stress to 100 MPa reduces the difference in the transient creep stage time and the minimum creep rate and, as a result, in the time to failure between the studied 12% Cr and 9% Cr steels. This is likely to be due to the elimination of advantages in the hardening of the 12% Cr steel with an increase
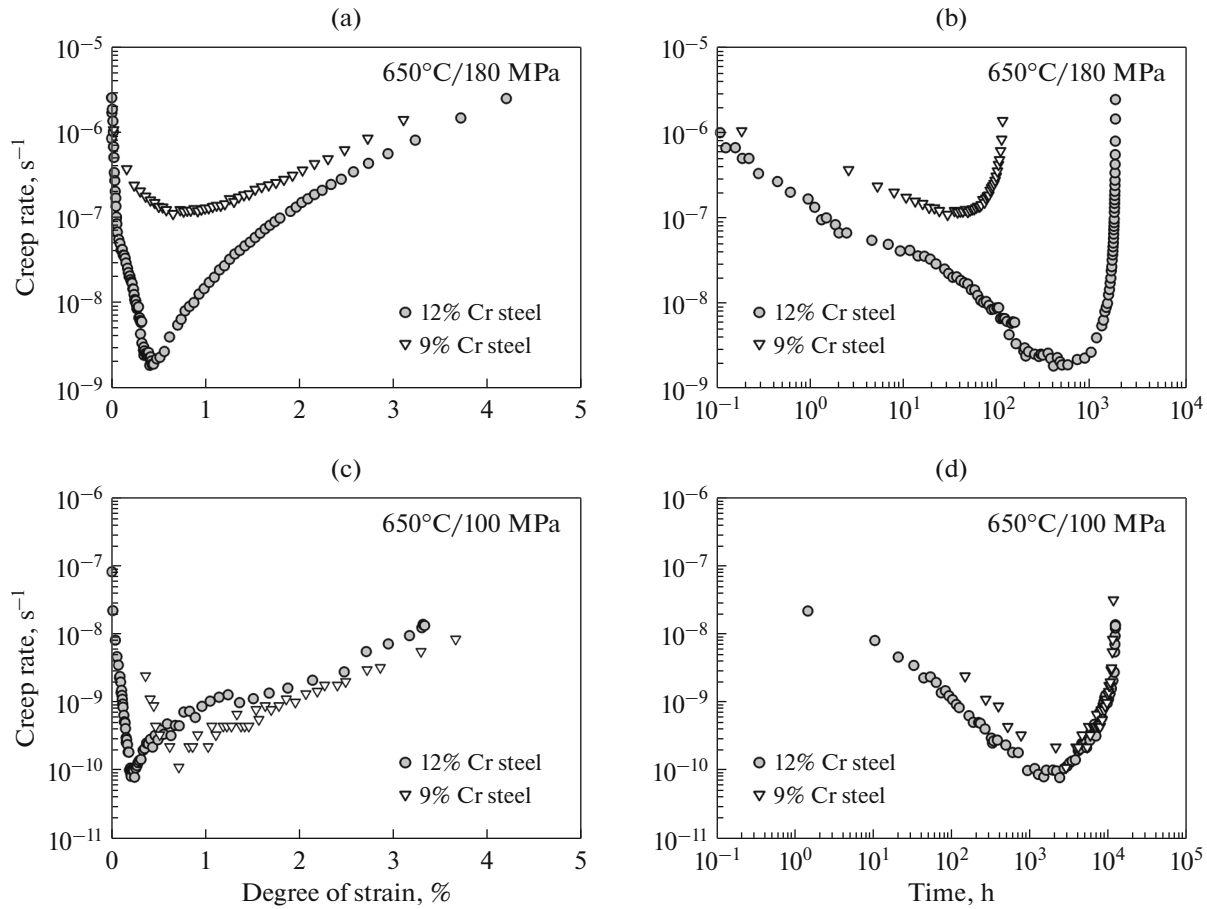
Fig. 4. Creep rate versus (a), (c) the degree of strain and (b), (d) time at a temperature of 650°C and applied stresses of (a), (b) 180, and (c), (d) 100 MPa for the studied 12% Cr and 9% Cr steels.

in the time of testing and the development of general processes, which make a contribution to failure of the material (coarsening of particles, transformation of the dislocation structure and substructure as a result of return).

The time to failure of the material is strongly related to the minimum creep rate at the established creep stage, and this is well described by the Monkman−Grant equation [1] (Fig. 5a)

$$\tau_r = (c'/\dot{\varepsilon}_{min})^{m'}, \qquad (1)$$

where τ_r is the time to failure of the material, h, $\dot{\varepsilon}_{min}$ is the minimum creep rate, h^{-1}, and c' and m' are constants. For both steels, it has been found that $c' = 0.28$ and $m' = 0.69$ under all creep conditions. No evidence has been found of deviations from the linear dependence of the minimum creep rate on the time to failure of the material within a range of studied strain rates from 10^{-2} to 10^{-7} h^{-1} for both studied steels.

The dependence of the applied stress on the time to failure of the material is shown in Fig. 5b. It was revealed after creep tests that the 9% Cr steel demon-

strates well-defined creep strength breakdown after 2000 h of creep testing, whereas the long-term strength curve of the 12% Cr steel has no such breakdown under the same creep conditions. In this case, the slope of the long-tern strength curve of the 12% Cr steel is higher than for the 9% Cr steel even after the breakdown point (Fig. 5b). A great increase in the time to failure of the material at high stresses of 200−140 PMa takes place due to some advantages in the solid-state and substructural hardening of the 12% Cr steel (Figs. 3 and 5b). A decrease in the applied stresses to 120−100 MPa reduces the advantages in the hardening of the 12% Cr steel to the level of the 9% Cr steel, thus evidencing that the 12% Cr steel has rather high structural stability, which is no worse than for the 9% Cr steel.

To estimate the applicability of the 12% Cr steel as a material for the manufacture of boiler, steam pipeline, and steam turbine blade elements, the 1% creep limit was calculated by the empirical dependence between the stress and the time required to attain the degree of strain at a level of 1% (Larson−Miller equation [1]):

$$P = T(\log t_{1\%} + 36) \times 10^{-3}, \qquad (2)$$
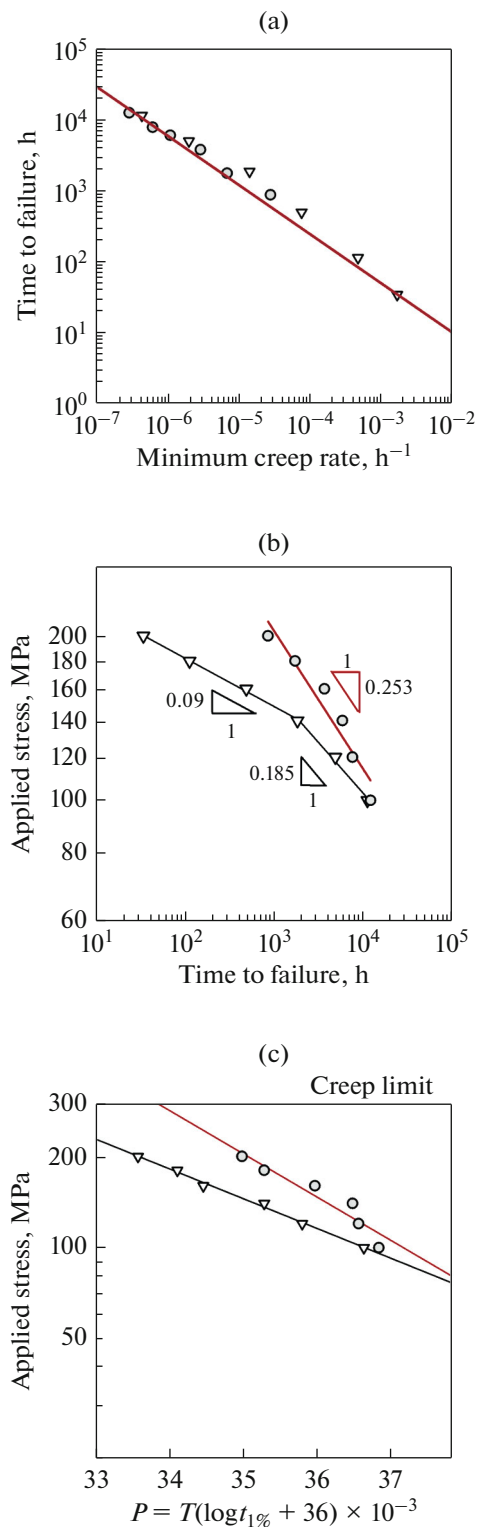
Fig. 5. (a) Minimum creep rate versus time to rupture, (b) applied stress versus time to rupture, and (c) calculation of the 1% creep limit with the Larson−Miller parameter; tests were performed at 650°C for the 12% Cr (○) and 9% Cr (▽) steels.

where P is the Larson−Miller parameter, T is the testing temperature, K, and $t_{1\%}$ is the time required to attain the degree of strain at a level of 1%, h. The dependences between the applied stress and the Larson−Miller parameters for the 12 and 9% Cr steels are shown in Fig. 5c. The creep limit of the 12% Cr and 9% Cr steels is 82 and 76 MPa, respectively. The comparable creep limit values indicate that the properties of the 12% Cr steel under creep are competitive with the properties of the 9% Cr steel. The developed chemical composition of the 12% Cr steel provides the possibility to overcome the major disadvantage of high-chromium steels, i.e., microstructural instability during creep, maximally approaching the properties of this steel under creep to the level of 9% Cr steel properties.

CONCLUSIONS

The mechanical properties of the 12% Cr and 9% Cr steel under tension and creep have been studied. The 12% Cr steel demonstrates an increase in the 1% creep limit and ultimate tensile strength at 20 and 650°C in comparison with the 9% Cr steel due to the improvement of solid-solution and substructural hardening. In the process of creep at high stresses of 200−140 MPa, a longer time to failure for the 12% Cr steel is caused by a more prolonged transient creep stage. A decrease in the applied stresses reduces the distinction in the creep behavior of the 12% Cr and 9% Cr steels. The 1% creep limit of the 12% Cr steel is 86 MPa, which evidences that the 12% Cr steel under creep has high microstructural stability comparable with the stability of 9% Cr steel.

REFERENCES

1. F. Abe, T. U. Kern, and R. Viswanathan, *Creep-Resistant Steels* (Woodhead Publishing, Cambridge, 2008), p. 800.

2. K. Kimura, "Creep strength of high chromium steel with ferrite matrix," Int. J. Pressure Vessels Piping **87**, 282−288 (2010).

3. R. O. Kaibyshev, V. N. Skorobogatykh, and I. A. Shchenkova, "New martensitic steels for fossil power plant:

creep resistance," Phys. Met. Metallogr. **109**, 186−200 (2010).

4. R. Viswanathan and W. Bakker, "Materials for ultrasupercritical coal power plants—boiler materials: Part 1," J. Mater. Eng. Perform. **10**, 81−95 (2001).

5. R. L. Klueh, "Elevated−temperature ferritic and martensitic steels and their application to future nuclear reactors," Int. Mater. Rev. **50**, 287−310 (2005).

6. M. Hattestrand, M. Schwind, and H.-O. Andren, "Microanalysis of two creep resistant 9−12% chromium steels," Metall. Mater. Trans. A. **250**, 27−36 (1998).

7. A. E. Fedoseeva, P. A. Kozlov, V. A. Dudko, A. N. Belyakov, V. N. Skorobogatykh, I. A. Shchenkova, and R. O. Kaibyshev, " Microstructural changes in steel 10Kh9V2MFBR during creep for 40000 hours at 600°C," Phys. Met. Metallogr. **116**, 1047−1056 (2015).

8. V. A. Dudko, A. E. Fedoseeva, A. N. Belyakov, and R. O. Kaibyshev, "Influence of the carbon content on the phase composition and mechanical properties of P92-type steel," Phys. Met. Metallogr. **116**, 1165−1174 (2015).

9. A. E. Fedoseeva, N. R. Dudova, and R. O. Kaibyshev, "Effect of stresses on the structural changes in high-chromium steel upon creep," Phys. Met. Metallogr. **118**, 591−600 (2017).

10. P. Jauhiainen, S. Yli-Oli, A. Nyholm, P. Auerkari, and J. Salonen, "Impact of oxidation on creep life of super-heaters and rehearters, creep&fracture in high temperature components," *2nd ECCC Creep Conference* (DEStech Publications, 2009), pp. 320−328.

11. I. Nikitin, A. Fedoseeva, and R. Kaibyshev, "Strengthening mechanisms of creep-resistant 12% Cr−3% Co steel with low N and high B contents," J. Mater. Sci. **55**, 7530−7545 (2020).

12. H. K. Danielsen, "Review of Z phase precipitation in 9−12 wt. % Cr steels," Mater. Sci. Technol. **32**, 126−137 (2016).

13. D. V. Edmonds and R. C. Cochrane, "Structure-property relationships in bainitic steels," Metall. Trans. A **21**, 1527−1540 (1990).

14. Q. Li, "Modeling the microstructure-mechanical property relationship for a 12% Cr−2W−V−Mo−Ni power plant steel," Mater. Sci. Eng., A **361**, 385−391 (2003).

15. C. E. Lacy and M. Gensamer, "The tensile properties of alloyed ferrites," Trans. ASME **9**, 118−125 (1944).

16. G. I. Taylor, "The mechanism of plastic deformation of crystals. Part I.-Theoretical," Proc. R. Soc. A **145**, 362−388 (1934).

17. F. J. Humphreys and M. Hatherly, *Recrystallization and Related Annealing Phenomena*, 2nd ed. (Elsevier, Amsterdam, 2004), p.658.

18. G. Langford and M. Cohen, "Strain hardening of iron by severe plastic deformation," ASM-Trans. **62**, 623−638 (1969).

19. J. P. Nailor, "The influence of the lath morphology on the yield stress and transition temperature of martensitic-bainitic steels," Metall. Trans. A **10**, 861−873 (1979).

Translated by E. Glushachenkova